RSC Advances

PAPER

View Article Online
View Journal | View Issue

Cite this: *RSC Adv.*, 2019, **9**, 5110

Synthesis and characterization of a surface-grafted Pb(II)-imprinted polymer based on activated carbon for selective separation and pre-concentration of Pb(II) ions from environmental water samples

Zhenhua Li,* Lihua Chen, Qiong Su, Lan Wu, Xiaohong Wei,* Liang Zeng and Muchen Li

Even the lowest concentration level of lead (Pb) in the human body is dangerous to health due to its bioaccumulation and high toxicity. Therefore, it is very important to develop selective and fast adsorption methods for the removal of Pb(II) from various samples. In this paper, a new Pb(II) ion-imprinted polymer (Pb(II)-IIP) was prepared with surface imprinting technology by using lead nitrate as a template, for the solid-phase extraction of trace Pb(II) ions in environmental water samples. The imprinted polymer was characterized by X-ray diffraction, Fourier transform infrared spectroscopy, Raman spectroscopy, scanning electron microscopy and N_2 adsorption–desorption isotherms. The separation/pre-concentration conditions for Pb(II) were investigated, including the effects of pH, shaking time, sample flow rate, elution conditions and interfering ions. Compared with non-imprinted particles, the ion-imprinted polymer had a higher selectivity and adsorption capacity for Pb(II). The pseudo-second-order kinetics model and Langmuir isotherm model fitted well with the adsorption data. The relative selectivity factor values (α_r) of Pb(II)/Zn(II), Pb(II)/Ni(II), Pb(II)/Co(II) and Pb(II)/Cu(II) were 168.20, 192.71, 126.13 and 229.39, respectively, which were all much greater than 1. The prepared Pb(II)-imprinted polymer was shown to be promising for the separation/pre-concentration of trace Pb(II) from natural water samples. The adsorption and desorption mechanisms were also proposed.

Received 5th December 2018
Accepted 25th January 2019

DOI: 10.1039/c8ra09992h

rsc.li/rsc-advances

Introduction

In recent years, water pollution caused by heavy metals has been one of the major economic and environmental problems all over the world. Among heavy metal ions, lead (Pb) is one of the most toxic for animals and humans. Through the food chain system of soil-plant-animal-human, Pb(II) is transferred into animals and human beings, causing severe contamination.[1] Therefore, the accurate and sensitive determination of Pb(II) in real samples is an important part of analytical chemistry. Reproducible, accurate and sensitive analytical methods are required for the determination of trace Pb in environmental samples. Among the spectral methods, inductively coupled plasma atomic emission spectrometry (ICP-OES) and atomic absorption spectrometry (AAS) are simple and rapid methods for the determination of metal ion concentrations,[2] however they are usually insufficiently sensitive due to matrix interferences and the very low concentration of metal ions present. Therefore, a separation/pre-concentration step is required.

Nowadays, the solid-phase extraction (SPE) technique is widely used for the pre-concentration of heavy metals due to its high enrichment factors, absence of emulsion formation, safety with respect to hazardous samples, minimal costs due to low consumption of reagents, flexibility and ease of automation.[3]

The choice of sorbent is an important factor in SPE because it can control the analytical parameters such as affinity, capacity and selectivity.[4] Activated carbon is known as the most traditional adsorbent for removal of organic and inorganic pollutants from aqueous as well as gaseous environments.[5] It is a widely used adsorbent in water and wastewater treatments due to its high surface area, environmentally friendly nature and because the methods are well developed. However, without any surface treatment, activated carbon presents an adsorption capacity for metal ions ranging from fair to zero, due to the fact that metal ions often exist in solution either as ions or as hydrous ionic complexes. On the other hand, chelating-agent modified activated carbons have been reported for the enrichment of metal ions.[6–9] Although remarkable adsorption capacities and adsorption rates may be achieved by using these

Key Laboratory of Environmental Friendly Composite Materials and Biomass Utilization, Chemical Engineering Institute, Northwest Minzu University, Lanzhou, China. E-mail: lizhh02006@163.com; weixh12@lzu.edu.cn; Fax: +86 931 4512932; Tel: +86 931 4512932

adsorbents, the adsorption selectivity for target metal ions remains unsatisfactory, which means that the adsorbents are unlikely to remove or enrich target metal ions from wastewater in the presence of many competitive ions. Recently, however, more and more extensive studies describing highly selective molecularly imprinted materials have been reported.[10–12]

Molecular imprinting is a method for the tailor-made preparation of highly selective synthetic polymer receptors for given molecules. The principle of molecular imprinting is that a target molecule (template) and functional monomers are polymerized with a crosslinking reagent. After removal of the template, the functional groups in the resulting binding sites should be arranged in positions suitable for subsequent interactions with template molecules[13] and so molecular imprinting polymers (MIPs) are capable of recognizing and binding the desired molecular target with a high affinity and selectivity.[14] An ion-imprinted polymer (IIP) is obtained when a metal ion is used as the template in the above-described synthesis. In most cases, specific ligands capable of forming a stable complex with the metal ion (or metal ion complexes with such specific ligands) are used in the polymerization process. The high selectivity of IIP can be explained by the polymer memory effect toward the metal ion interaction with a specific ligand, coordination geometry, metal ion coordination number, charge and size.[15] One potential application of IIPs that has recently attracted widespread interest is the clean-up and enrichment of analytes present at low concentrations in complex matrices.[16,17] Many studies on IIPs and their use for selective separation and pre-concentration of metal ions have been reported.[18–21] However, as far as we know, there has been no report on using a surface-imprinted activated carbon sorbent for Pb(II) enrichment.

Ethylenediamine has stable physical and chemical properties, and is commonly used as complexing agent. Based on this, in this work, ethylenediamine was selected as the functional monomer, epichlorohydrin was selected as the cross-linker, and a new and green Pb(II)-IIP was prepared by the surface molecular imprinting technique for the removal of Pb(II) ions from aqueous solutions. The proposed method presented high adsorption capacity and selectivity for Pb(II), and offered a convenient, accurate and simple route to the clean-up of water samples.

Experimental

Apparatus

An Iris Advantage ER/S inductively coupled plasma emission spectrometer, (Thermo Jarrel Ash, Franklin, MA, USA) was used for the determination of all metal ions. The instrumental parameters were those recommended by the manufacturer. The wavelength selected for Pb was 216.999 nm. Infrared spectra (4000–400 cm^{-1}) in KBr were recorded on a Nicolet NEXUS 670 FT-IR apparatus (USA). Raman spectra were measured with a 532 nm edge by using a LabRAM HR Evolution spectrometer (HORIBA Jobin Yvon S.A.S.) A JSM-6701F (JEOL, Japan) was used to obtain scanning electron microscopy (SEM) images. A Philips X'pert diffractometer with Cu K_α radiation (Holland) was used to acquire the X-ray diffraction (XRD) patterns of powdered samples. N_2 adsorption–desorption isotherms (Brunauer–Emmett–Teller; BET) were measured using a TriStar II 3020 V1.04 apparatus (USA). The pH values were controlled with a pHs-3C digital pH meter (Shanghai Lei Ci Device Works, China). A YL-110 peristaltic pump (General Research Institute for Non-ferrous Metals, Beijing, China) was used in the separation/pre-concentration process. A polytetrafluoroethylene (PTFE) column (50 mm × 9.0 mm i.d.) (Tianjin Jinteng Instrument Factory, Tianjin, China) was used.

Chemicals and reagents

Standard stock solutions of Pb(II), Zn(II), Ni(II), Co(II) and Cu(II) (1 mg mL^{-1}) were prepared by dissolving appropriate amounts of analytical grade salts in double distilled water (DDW) with the addition of 1.0% HNO_3, and they were further diluted daily prior to use. Activated carbon (AC, 40–60 mesh) was provided by Tianjin Guangfu Fine Chemical Research Institute, Tianjin, China. It was dried in a vacuum at 110 °C for 48 h before use. Ethylenediamine (EN), thiourea and *N*,*N*′-dicyclohexylcarbodiimide (DCC) were purchased from Sinopharm Chemical Reagent Co., Ltd. (Beijing, China). Epichlorohydrin (EIN) was provided by Shenyang Xinxing Reagent Factory (Shenyang, China). The certified reference materials (GBW 08301: river sediment; GBW 08303: polluted farming soil) were obtained from the National Research Center for Certified Reference Materials (Beijing, China).

Sample preparation

The river water samples were collected from Yellow River (Chengguan district of Lanzhou, China) and Huangshui River (Centre Square of Xining, China). Lake water was collected from South Lake, Lanzhou, China. The water samples were filtered through a 0.45 μm PTFE millipore filter, and acidified to a pH of about 2 with concentrated HCl prior to storage for use. Tap water samples taken from our research laboratory were analyzed without any pretreatment. The pH value was adjusted to 2 with 0.1 mol L^{-1} HCl prior to use.

The certified reference materials (GBW 08301: river sediment; GBW 08303: polluted farming soil) were digested according to the literature methods.[22]

Synthesis

Preparation of carboxylic derivative of activated carbon (AC-ACOOH). The activated carbon (AC) was first purified and activated with 10% (v/v) HCl solution for 24 h in order to remove the metal ions and other impurities sorbed on it. Then 10 g of the purified AC was suspended in 300 mL of 32.5% (v/v) HNO_3 solution with heating and stirring for 5 h at 60 °C. The mixture was filtered, washed with deionized water to neutral, and dried under vacuum at 80 °C for 8 h. The product was the carboxylic derivative of activated carbon (AC-ACOOH).

Preparation of the Pb(II) imprinted and non-imprinted polymers. The Pb(II)-imprinted activated carbon polymer (Pb(II)-IIP) was prepared by the procedure shown in Fig. 1. Firstly, 2.782 g of $Pb(NO_3)_2$ was dissolved in 80 mL of ethanol

with stirring and heating, and then 3 mL of ethylenediamine (EN) was added into the mixture. The solution was stirred and refluxed for 1 h. In this process, functional monomers (EN) and template ions (Pb(II)) were preassembled. Secondly, 6 g of AC-COOH and 2 mL of epichlorohydrin (EIN) were added into the mixture, after which, 5.0 g of *N*,*N*-dicyclohexylcarbodiimide (DCC) was slowly added and the suspension was refluxed for 48 h. In this process, EIN was used as the cross-linker and DCC was used as the condensation agent. Lastly, the product was recovered by filtration, washed with ethanol and stirred for 10 h in 100 mL of 0.04 mol L^{-1} HCl to remove Pb(II) ions. The final product was cleaned with DDW and then dried under vacuum at 70 °C for 12 h. The non-imprinted polymer (Pb(II)-NIP) was prepared using an identical procedure except that $Pb(NO_3)_2$ was not added.

Procedures

Static procedure. A portion of a standard or sample solution containing Pb(II) was transferred to a 10 mL beaker, and the pH value was adjusted to the desired value with 0.1 mol L^{-1} HNO_3 or 0.1 mol L^{-1} $NH_3 \cdot H_2O$. Then the volume was adjusted to 10 mL with deionized DDW. Pb(II)-IIP or Pb(II)-NIP (30 mg) was added, and the mixture was mechanically shaken for 30 min to attain equilibrium. After the solution was centrifuged, the concentrations of the metal ions in the solution were directly determined by ICP-AES. The adsorption capacity, distribution ratio, selectivity coefficient and relative selectivity coefficient were calculated according to the following equations:

$$Q = \frac{(C_o - C_e)V}{W}$$

$$E\% = \frac{(C_o - C_e)}{C_o} \times 100\%$$

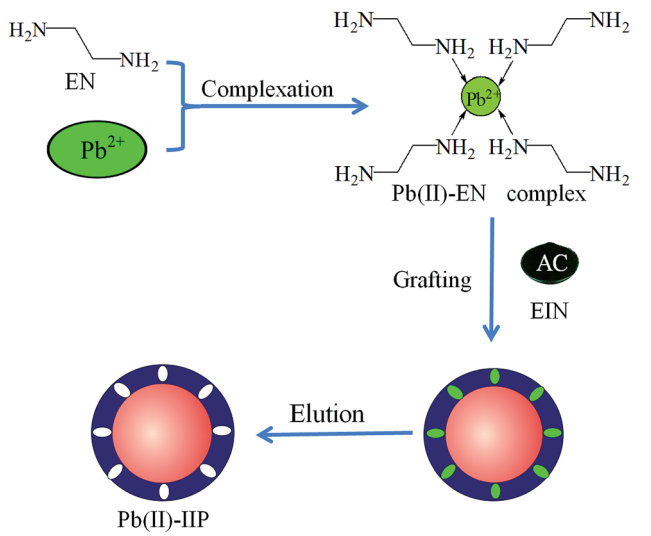

Fig. 1 Scheme for the preparation of Pb(II)-IIP.

$$D = \frac{Q}{C_e}$$

$$\alpha = \frac{D_{Pb}}{D_M}$$

$$\alpha_r = \frac{\alpha_i}{\alpha_n}$$

where Q represents the adsorption capacity (mg g^{-1}), C_o and C_e represent the initial and equilibrium concentrations of Pb(II) (μg mL^{-1}), W is the mass of Pb(II)-imprinted amino-functionalized AC polymer (g), V is the volume of metal ion solution (L), E% is the extraction percentage, D is the distribution ratio (mL g^{-1}), D_{Pb} and D_M represent the distribution ratios of Pb(II) and Ni(II), Co(II), Zn(II), or Cu(II) respectively, α is the selectivity coefficient, α_r is the relative selectivity coefficient, and α_i and α_n represent the selectivity factors of Pb(II)-IIP and Pb(II)-NIP, respectively.

Dynamic procedure. Functionalized Pb(II)-IIP (30 mg) was packed into a PTFE column which was plugged with a small portion of glass wool at both ends. Before use, 0.1 mol L^{-1} HCl and deionized DDW were successively passed through the microcolumn in order to equilibrate, clean and neutralize it. A suitable aliquot of the sample solution containing 1.0 μg mL^{-1} Pb(II) in a volume of 50 mL was adjusted to pH 4.0 and passed through the column at a flow rate of 3.0 mL min^{-1} under the control of a peristaltic pump. The bound metal ions were stripped off from the gel column with 0.04 mol L^{-1} HCl solution. The concentration of the metal ions in the eluate was determined by ICP-AES.

Results and discussion

Characteristics of the imprinted polymer

FT-IR spectra. The modification of the AC was confirmed by FT-IR analysis (Fig. 2). When the FT-IR spectrum of AC-COOH was compared with that of AC, a new band (1706 cm^{-1}) appeared due to the C=O stretching vibration of the carboxylic acid group, which indicated that the carboxylic derivative of AC had been prepared successfully. Several new peaks also appeared in the spectrum of Pb(II)-IIP. According to the literature,[23,24] the new peaks could be assigned as follows: the peak at 1702 cm^{-1} was due to C=O stretching vibrations; the peak at 1567 cm^{-1} was caused by N–H bending vibrations; and the bands around 3430 cm^{-1} could be assigned to N–H stretching vibrations. The main bands of the spectra of Pb(II)-IIP and Pb(II)-NIP showed very similar locations and appearances. This indicated that N–H was recovered after removal of Pb(II) in the imprinted sorbent. These results suggested that $-NH_2$ had been grafted onto the surface of the AC after modification.

Raman spectroscopy. Raman spectroscopy is a powerful tool for characterizing carbonaceous materials due to their high Raman intensity.[25] Fig. 3 shows the Raman spectra of AC, AC-COOH and Pb(II)-IIP. Two prominent peaks were clearly observed at around 1350 and 1600 cm^{-1}, corresponding to the D

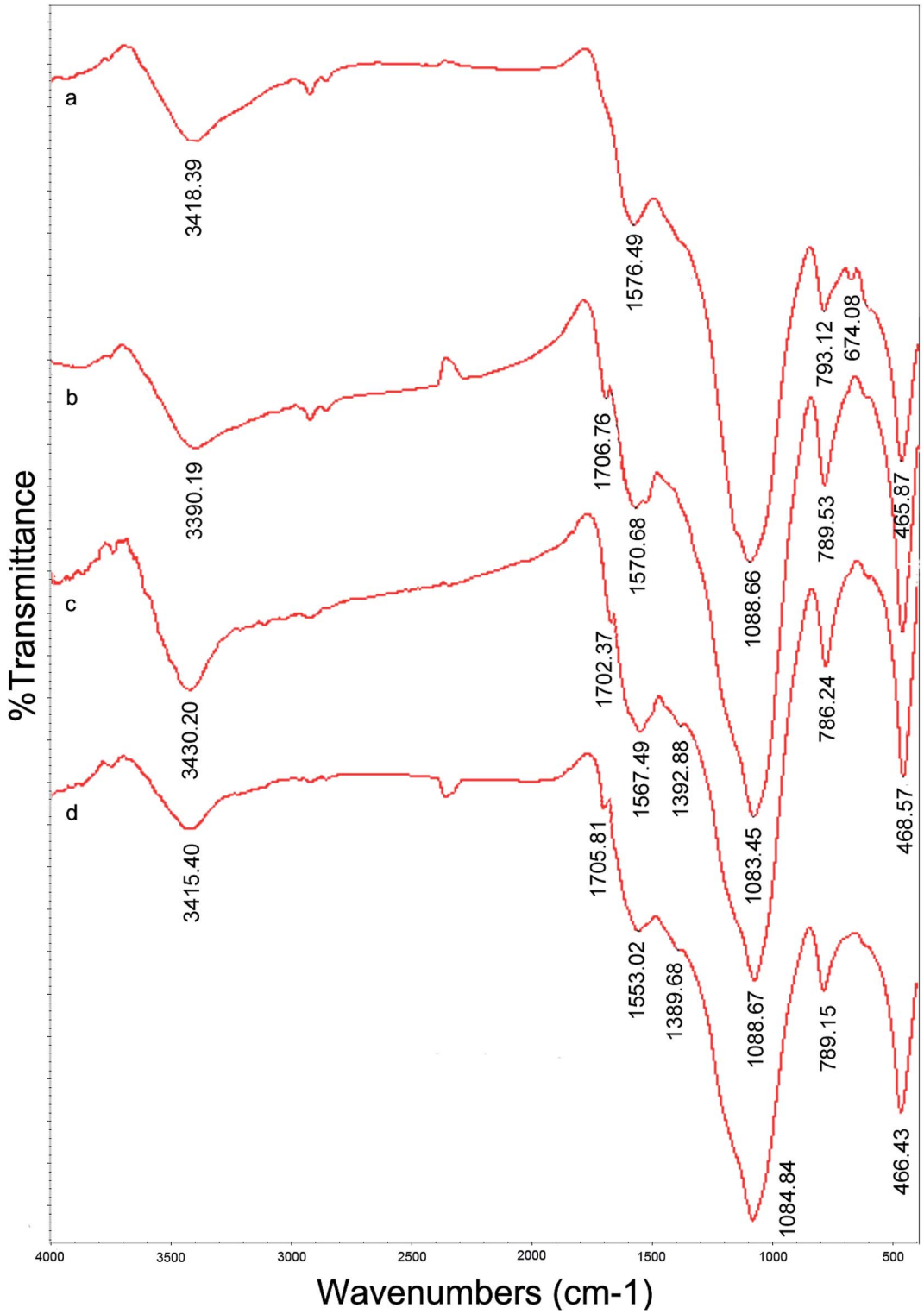

Fig. 2 FT-IR spectra of AC (a), AC-COOH (b), Pb(II)-IIP (c) and Pb(II)-NIP (d).

peak (resulting from a disordered sp^3 carbon structure) and the G peak (representing sp^2 ordered crystalline graphite-like structures), respectively. The intensity ratio (I_D/I_G) is characteristic of the extent of disorder present within a material.[26] The calculated I_D/I_G ratios of AC, AC-COOH, and Pb(II)-IIP were 0.827, 0.884 and 0.968, respectively, indicating an increase in disorder. Compared with AC, the increased ratio for AC-COOH may be attributed to the carboxylation of AC. Similarly, the increase in the I_D/I_G ratio for Pb(II)-IIP might be ascribed to the covalent interaction of AC-COOH with the amino groups and

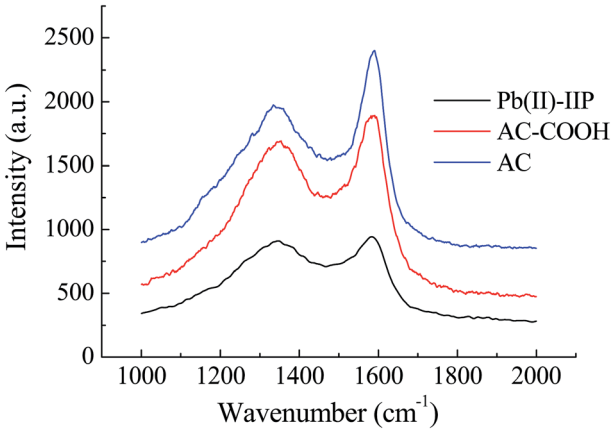

Fig. 3 Raman spectra of AC, AC-COOH and Pb(II)-IIP.

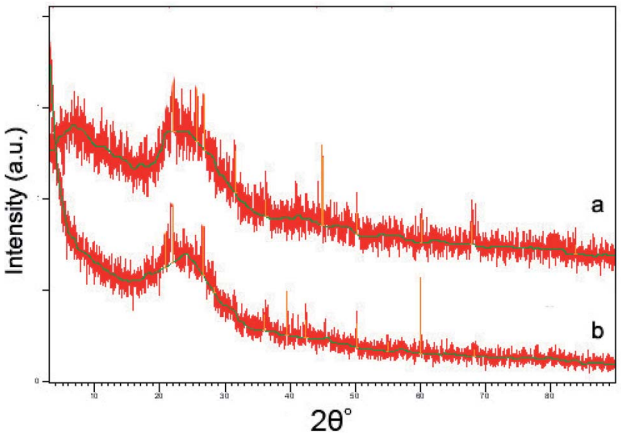

Fig. 5 XRD patterns of AC (a) and Pb(II)-IIP (b).

IIP. All these results suggested that Pb(II)-IIP was successfully synthesized.

SEM images. SEM was conducted to characterize the AC, AC-COOH and Pb(II)-IIP. The representative SEM images are shown in Fig. 4. The AC formed a dense and robust structure (see Fig. 4a). Compared with AC, AC-COOH (see Fig. 4b) showed a greater degree of microstructure and the specific surface area was increased. It can be observed in Fig. 4c that the surface structure of Pb(II)-IIP was also changed obviously, and the micro structure was more bulky. Pb(II)-IIP had a rich network of hole structures which could be applied for the enrichment of Pb(II).

XRD patterns. To clarify the crystal structure of AC and Pb(II)-IIP, XRD was carried out and the results are shown in Fig. 5. Obviously, the diffraction peaks around the angle of 23° were related to the surface planes (002) of quasi graphitoid microcrystals. After the surface imprinting treatment, the intensity of the (002) diffraction peak was weakened, showing a wider and shorter characteristic. No other obvious diffraction peaks were found in the patterns, indicating that the degree of crystallization of the two materials was not very high.

BET analysis. In addition, the results of the BET analysis showed that the specific surface area and pore volume of AC were 100.7967 $m^2\ g^{-1}$ and 0.11 $cm^3\ g^{-1}$, respectively. Compared to AC, Pb(II)-IIP presented lower values for both the surface area (76.7967 $m^2\ g^{-1}$) and pore volume (0.08 $cm^3\ g^{-1}$), which was attributed to the modification of AC achieved at the expense of porosity and specific surface area.[27]

Effect of pH. One of the most important parameters influencing the efficiency of retention of an analyte on a sorbent is the pH of the sample. The effect of varying pH values on Pb(II) uptake was investigated using the recommended procedure (static method). The solutions were enriched at pH values ranging from 1–7 and then analyzed by ICP-AES. It can be seen from Fig. 6 that Pb(II) could be adsorbed quantitatively on Pb(II)-IIP within the pH range of 3–7. In order to avoid hydrolysis at higher pH values, pH 4 was selected as the enrichment acidity for subsequent work.

Effect of elution conditions on recovery. Elution of Pb(II) from the microcolumn containing the Pb(II)-IIP was carried out using various concentrations and volumes of thiourea and HCl eluents following the general procedure (dynamic method).

From the data given in Table 1, it is obvious that quantitative elution was not obtained by using thiourea alone as the desorption reagent (recovery < 60%). When HCl was used as the desorption agent, the coordination spheres of chelated Pb(II) were disrupted and subsequently Pb(II) ions were released from the lead templates into the desorption medium. Quantitative recoveries (>95%) of Pb(II) could be obtained using 2 mL of 0.04 mol L^{-1} HCl solution as the eluent. Therefore, 2 mL of

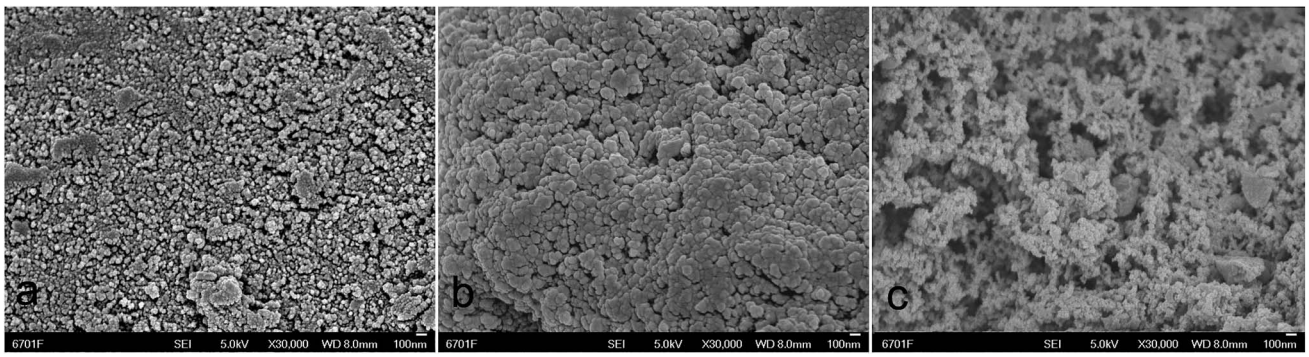

Fig. 4 SEM images of AC (a), AC-COOH (b) and Pb(II)-IIP (c).

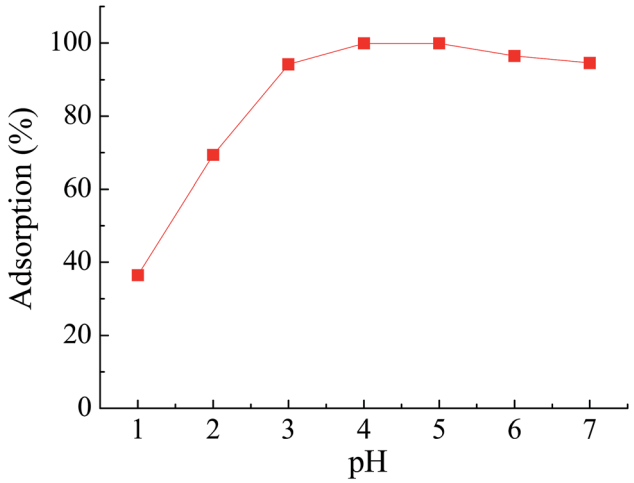

Fig. 6 Effect of pH on the adsorption of Pb(II) on Pb(II)-IIP.

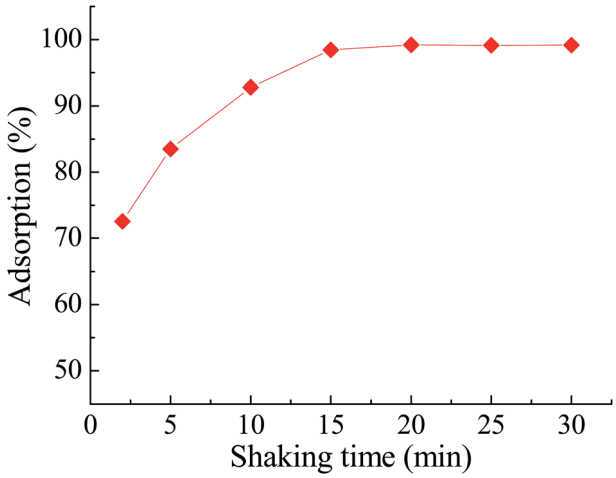

Fig. 7 Effect of shaking time on the adsorption of Pb(II) on Pb(II)-IIP. Other conditions: pH 4.0, temperature 25 °C.

0.04 mol L^{-1} HCl was used as the eluent in subsequent experiments.

Adsorption kinetics study. The effect of shaking time on the percentage extraction of metal ions is considered to be very important because it determines the possible discrimination in the behavior of the new synthesized phases towards different metal ions. In this work, different shaking times (ranging from 5 to 40 min) were studied for the percentage extraction of Pb(II) by Pb(II)-IIP. The results (Fig. 7) showed that the level of Pb(II) uptake was found to increase rapidly with the increase in contact time during the first 15 min and then a plateau was reached at equilibrium. This could be attributed to the fact that there were a large number of adsorption sites on the sorbent surface, which were available for the adsorption of Pb(II) ions during the early stage. This indicated that the surface imprinting greatly facilitated the diffusion of Pb(II) to the binding sites and that the adsorption was a rapid kinetic process. We selected 15 min shaking time for further studies.

In order to investigate the factors influencing the adsorption rate, it is necessary to study the kinetics of the adsorption process. Pb(II)-IIP (30 mg) was allowed to interact with 10 mL of Pb(II) solution (400 ug mL^{-1}) for periods of 15–120 min.

Therefore, the kinetic changes in this study were evaluated using the pseudo-first-order kinetic model (1) and pseudo-second-order kinetic model (2):

$$\ln(Q_t - Q_e) = -K_1 t + \ln Q_e \quad (1)$$

$$\frac{t}{Q_t} = \frac{t}{Q_e} + \frac{1}{K_2 Q_e^2} \quad (2)$$

where Q_e and Q_t represent the adsorption capacity at equilibrium and at the time t (mg g^{-1}) respectively, K_1 represents the rate constant of pseudo-first-order adsorption (min^{-1}), and K_2 represents the rate constant of pseudo-second-order adsorption (g mg^{-1} min^{-1}).

The kinetics parameters for Pb(II) adsorption are listed in Table 2. The correlation coefficients (R^2) of the pseudo-second-order equation were higher than those of the pseudo-first-order equation. Also, the calculated Q_e values were in better agreement with the experimental results for the pseudo-second-order kinetic model, indicating its better suitability for describing the adsorption kinetics of Pb(II) onto Pb(II)-IIP. The good fit to the pseudo-second-order kinetic model could imply that the predominant adsorption process was chemisorption. The results also suggested that Pb(II) ions could combine with active sites on the Pb(II)-IIP *via* covalent chemical bonding.[28] The results could be expected because the polymerization reactions occurred only on the AC.

Effect of flow rate. Another important parameter in adsorption is the flow rate of the sample solution, which influences the adsorption of cations to the sorbent surface in the time of analysis. Therefore, the effect of the flow rate of sample solutions was examined under the optimum conditions by passing 10 mL sample solutions through the column with a peristaltic pump. The flow rates were adjusted in the range of 0.5 to 5.0 mL min^{-1}. It can be seen from Fig. 8 that the retention of Pb(II) was practically unchanged up to a flow rate of 3.0 mL min^{-1}.

Table 1 Eluent recovery (%) for Pb(II) adsorbed on Pb(II)-IIP ($N = 3$)

Optimization of eluent type and concentration ($V = 10$ mL)		
Eluent type	Concentration of eluent	Recovery (%)
Thiourea	0.01 M	42.47
	0.05 M	58.09
HCl	0.01 M	90.74
	0.02 M	94.82
	0.03 M	98.35
	0.04 M	99.42
	0.05 M	99.11

Optimization of eluent volume ($C = 0.04$ mol L^{-1} HCl)						
Eluent volume (mL)	1.0	1.5	2.0	2.5	3.0	4.0
Recovery (%)	86.65	96.16	100	100	100	100

Table 2 Parameters of different kinetic models for the adsorption process

First-order model			Second-order model		
K_1 (min^{-1})	Q_e (mg g^{-1})	R^2	K_2 (g mg^{-1} min^{-1})	Q_2 (mg g^{-1})	R^2
0.041	3.64	0.779	0.036	90.90	0.999

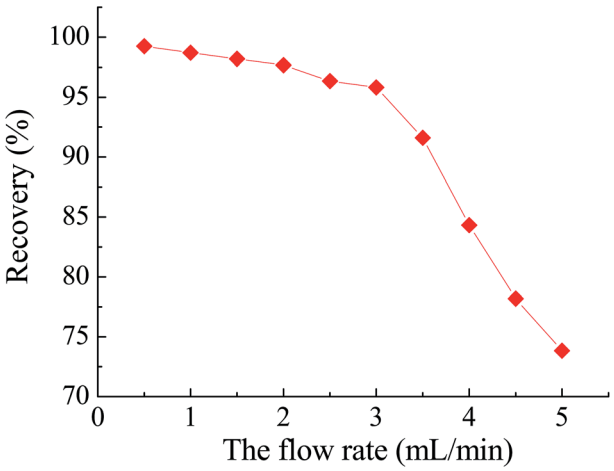

Fig. 8 Effect of solution flow rate on the recovery of Pb(II). Other conditions: volume 50 mL, pH 4.0, temperature 25 °C.

The recovery of Pb(II) decreased slightly when the flow rate was over 3.0 mL min^{-1}. Thus, a flow rate of 3.0 mL min^{-1} was selected in this work.

Maximum sample volume and enrichment factor. To explore the possibility of adsorbing low concentrations of analytes from large volumes of solution, the effect of sample volume on the retention of metal ions was investigated. For this purpose, different volumes of purified water at pH 4.0 were spiked with Pb(II) at a concentration level of 1.0 μg mL^{-1}. Following the experimental procedure, the recoveries of analyte from different volumes were obtained. The experimental results showed that a maximum sample volume of 400 mL gave a recovery of >95%. Therefore, 400 mL of sample solution was adopted for the preconcentration of Pb(II) from sample solutions, and a high enrichment factor of 200 was obtained when 2 mL of 0.04 mol L^{-1} HCl was used as the eluent in these experiments.

Effect of coexisting ions. The effects of common coexisting ions were investigated. In these experiments, solutions of 1.0 μg mL^{-1} of Pb(II) with added interfering ions were treated according to the procedure described for the batch adsorption test. The tolerance of the coexisting ions is defined by the amount that reduces the recovery of the studied element to less than 90%. It can be seen (Table 3) that the presence of major cations and anions had no obvious influence on the determination of Pb(II) under the selected conditions, which showed that the Pb(II)-IIP had a good selectivity for Pb(II) and was suitable for the analysis of samples with complicated matrices. There are three possible reasons for the selectivity of Pb(II).[29] One is the inherent selectivity of the amino-functionalized group: the amino group is a soft base that would not interact

Table 3 Effect of coexisting ions on the recovery of 1.0 μg mL^{-1} Pb(II) ($N = 3$)

Ion	Concentration (μg mL^{-1})	Added as	Recovery (%)
K^+	2000	KCl	100
Na^+	2000	NaCl	100
Mg^{2+}	1000	$MgSO_4$	96.45
Ca^{2+}	1000	$CaCl_2$	97.24
Cd^{2+}	100	$Cd(NO_3)_2 \cdot 4H_2O$	98.18
Cr^{3+}	100	$CrCl_3$	96.38
Co^{2+}	100	$CoCl_2$	96.35
Fe^{3+}	100	$FeCl_3$	94.23
Mn^{2+}	100	$MnSO_4 \cdot H_2O$	91.90
Ni^{2+}	100	$NiCl_2 \cdot 6H_2O$	93.82
Zn^{2+}	100	$ZnCl_2$	97.01
Hg^{2+}	100	$HgCl_2$	96.87
SO_4^{2-}	3000	Na_2SO_4	96.75
NO_3^-	3000	$NaNO_3$	99.18
Cl^-	3000	NaCl	92.42
F^-	3000	NaF	99.17

with alkali metal and alkali earth metal ions that are classified as hard acids. The second is the hole-size selectivity: the size of Pb(II) exactly fits the cavity of the Pb(II)-IIP. The third is the selectivity of the coordination-geometry: the Pb(II)-IIP can provide ligand groups which are arranged in the way required for coordination of Pb(II). Although some ions have similar sizes to Pb(II), and some ions have high affinity to the amino ligand, the Pb(II)-IIP still exhibited high selectivity for extraction of Pb(II) in the presence of other metal ions. These results suggested that the coordination-geometry selectivity might dominate in the enhancement of selectivity.

Adsorption capacity of Pb(II)-IIP for Pb(II). The adsorption capacity is an important factor because it determines how much sorbent is required to quantitatively concentrate the analytes from a given solution. The capacity study was modeled on the paper by Maquieira *et al.*[30] Pb(II)-IIP or Pb(II)-NIP (30 mg) was equilibrated with 10 mL of various concentrations (50–500 μg mL^{-1}) of Pb(II) solutions buffered with 0.1 mol L^{-1} of HNO_3 or $NH_3 \cdot H_2O$ at pH 4. A breakthrough curve was gained by plotting the concentration (μg mL^{-1}) *versus* the number of micrograms of Pb(II) adsorbed per gram of sorbent. From the breakthrough curve (Fig. 9), the maximum adsorption capacities of the Pb(II)-IIP and Pb(II)-NIP for Pb(II) were found to be 90.14 and 21.15 mg g^{-1}, respectively. The adsorption capacity of the Pb(II)-IIP was about four times that of the Pb(II)-NIP. The results showed that the Pb(II)-IIP had a high adsorption capacity for Pb(II). This difference indicated that imprinting plays an important role in the adsorption behavior. During the

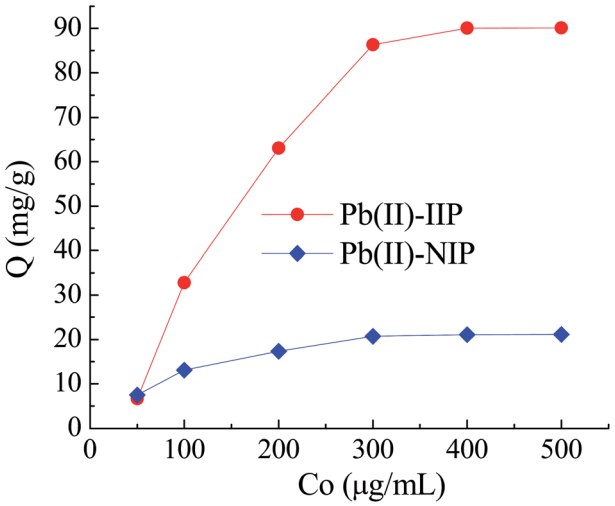

Fig. 9 Effect of initial concentration (C_o) of Pb(II) on the adsorption quantity (Q) of Pb(II)-IIP and Pb(II)-NIP. Other conditions: pH 4.0, temperature 25 °C.

preparation of the Pb(II)-IIP, the presence of Pb(II) made the ligands arrange in an orderly way. After the removal of Pb(II), the imprinted cavity and specific binding sites of the functional groups were formed in a predetermined orientation, whereas no such specificity was found in Pb(II)-NIP.

The adsorption process is normally described by the Langmuir isotherm. The Langmuir isotherm is valid for monolayer adsorption onto a surface containing a finite number of homogeneous sites. The Langmuir equation is expressed as follows (3):[31]

$$\frac{C_e}{Q_e} = \frac{C_e}{Q} + \frac{1}{Q_b}. \quad (3)$$

The plot of C_e/Q_e *versus* C_e gave a straight line ($R^2 = 0.999$) with a slope of $1/Q$ and an intercept of $1/Q_b$ which confirmed the validity of the Langmuir model for this process (Fig. 10).

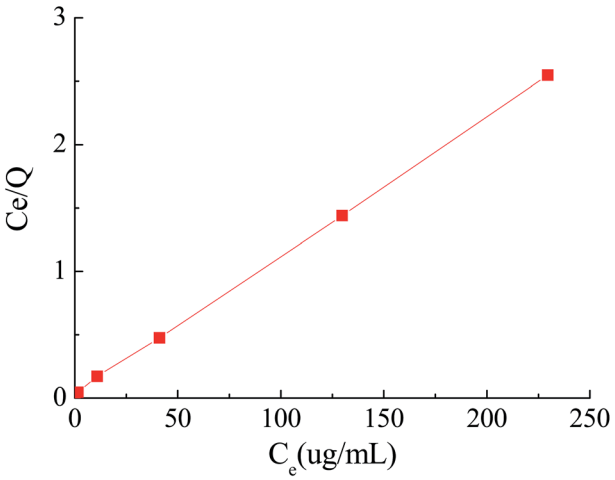

Fig. 10 The linearized form of the Langmuir adsorption isotherm. Other conditions: 30 mg Pb(II)-IIP, temperature 25 °C, pH 4.0.

Table 4 Competitive loading of Pb(II) with Ni(II), Co(II), Zn(II) and Cu(II) ions by the Pb(II)-IIP and Pb(II)-NIP

	E (%)		D (mL g^{-1})		α		
Metal ions	Imprinted	Non-imprinted	Imprinted	Non-imprinted	α_i	α_n	α_r
Pb(II)	99.70	59.77	122 213.24	495.18			
Zn(II)	52.56	42.97	368.44	251.11	331.70	1.972	168.20
Ni(II)	55.90	49.74	422.78	329.95	289.07	1.500	192.71
Co(II)	56.35	39.75	430.25	219.92	284.05	2.252	126.13
Cu(II)	59.61	57.84	491.95	457.33	248.43	1.083	229.39

Selectivity of the imprinted sorbent. In order to evaluate the selectivity of the imprinted sorbent, the competitive enrichments of Pb(II)/Zn(II), Pb(II)/Ni(II), Pb(II)/Co(II) and Pb(II)/Cu(II) from their mixtures were investigated in a static procedure because these five ions all have the same charge and similar ionic radii. In the binary mixtures, the two metal ions had the same concentrations of 5 μg mL^{-1} and the sorbent was 30 mg. As can be seen in Table 4, the distribution ratio (D) values of Pb(II)-IIP for Pb(II) were greatly higher than those of the other metals. The relative selectivity factor values (α_r) of Pb(II)/Zn(II), Pb(II)/Ni(II), Pb(II)/Co(II) and Pb(II)/Cu(II) were 168.20, 192.71, 126.13 and 229.39, respectively, which were all much greater than 1. The results indicated that the Pb(II)-IIP had high selectivity for Pb(II). This means that Pb(II) can be determined even in the presence of Zn(II), Ni(II), Co(II) and Cu(II).

Stability tests. To investigate the stability and the potential regeneration of the sorbent, the experiments of desorption and adsorption of Pb(II) were repeated eight times. After each test, the sorbents were washed with 0.04 mol L^{-1} HCl for recycling. As illustrated in Fig. 11, the adsorption capacity of Pb(II)-IIP showed no obvious decline with cycling. After eight cycles, the adsorption capacity of Pb(II)-IIP had decreased slightly from 90.13 to 87.09 mg g^{-1}, which mainly resulted from the mass loss of imprinted materials in the cycling processes. Herein, the reusability of Pb(II)-IIP was satisfactory; potentially it could be reused in water treatment.

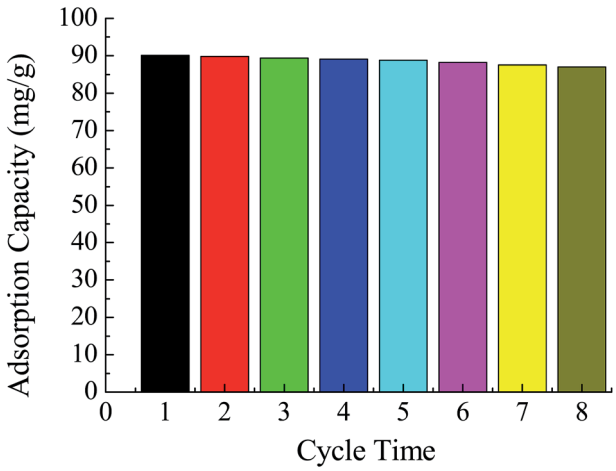

Fig. 11 Adsorption capacity of Pb(II)-IIP after eight cycles.

Table 5 Analysis results for the determination of Pb(II) in standard reference materials ($N = 3$)

Analytes	Measured ($\mu g\ g^{-1}$)	Certified ($\mu g\ g^{-1}$)
GBW 08301	79.2 ± 6.7	79 ± 12.0
GBW 08303	73.4 ± 1.3	73 ± 2.0

Table 6 Analytical results for the determination of Pb(II) in natural water samples

Ion	Added	Found [a]	Recovery (%)
Pb(II) ($\mu g\ mL^{-1}$)			
Yellow River water	0	6.49 ± 0.22	
	5	11.65 ± 0.05	101.4
	10	16.56 ± 0.12	100.6
Huangshui River	0	2.07 ± 0.09	
	5	7.13 ± 0.11	100.5
	10	12.04 ± 0.15	99.7
South Lake	0	3.86 ± 0.08	
	5	8.69 ± 0.07	98.1
	10	13.74 ± 0.13	99.1
Tap water	0	4.14 ± 0.08	
	5	9.12 ± 0.21	99.8
	10	14.33 ± 0.14	101.3

[a] The value following "±" is the standard deviation ($N = 3$).

Analytical precision and accuracy of the proposed method. Under the selected conditions, 11 standard solutions were analyzed simultaneously following the general procedure. The result showed that the relative standard deviation (RSD) was 2.2%, which indicated that the method had good precision for the analysis of trace Pb(II) in solution samples. The detection limit (blank + 3σ), as defined by International Union of Pure and Applied Chemistry (IUPAC), was found to be 0.18 $\mu g\ L^{-1}$.

The presented method was applied to the determination of trace Pb(II) in standard materials (GBW 08301: river sediment; GBW 08303: polluted farming soil) for validation. The analytical results for the certified reference materials (Table 5) were in good agreement with the certified values.

For the analysis of Yellow River water, Huangshui water, South Lake water and tap water samples, the standard addition method was used. The results are given in Table 6. It was found that the recoveries of analyte were in the range of 98–102%. Evidently, the obtained results indicated that the method was reliable, feasible and satisfactory for the analysis of water samples.

Comparison with other methods for the determination of Pb(II). The analytical characteristics of the method using Pb(II)-IIP for the determination of Pb(II), such as the flow rate, the equilibrium time, the enrichment factor, the number of cycles the material can be used, the selectivity and RSDs, and the adsorption capacity were compared with those of the other reported methods (Table 7). As seen from the data, the present method possesses advantages such as the recyclability of the material over considerably more cycles, faster attainment of equilibrium, higher selectivity, higher adsorption capacity and larger enrichment factor.

Adsorption mechanism. As described previously, Pb(II) adsorption onto Pb(II)-IIP could be fitted well by the pseudo-second-order kinetic model. This kinetic model indicates chemical reaction mechanisms, which include ion-exchange, adsorption, chemisorption and chelation.

A plausible adsorption mechanism of Pb(II) on Pb(II)-IIP is shown in Fig. 12 and is proposed as follows. Nitrogen atoms of Pb(II)-IIP have a lone pair of electrons that could bind with the electron deficient Pb(II) ions *via* chelation. Therefore, each divalent Pb(II) ion could bind to four nitrogen atoms to form

Table 7 Comparison of figures of merit for the determination of Pb(II)

Sorbent	ET[a] (min)	FR[b] (mL min^{-1})	Q (mg g^{-1})	EF[a]	LOD (ng mL^{-1})	Number of cycles	RSD (%)	Selectivity	Ref.
Pb(II)-imprinted silica gel	30	1	19.66	100	0.004	—	<2.0	Pb	32
Co_3O_4	—	—	35.5	175	0.72	—	1.5	Pb	33
Pb(II)-imprinted polymer in nano-TiO_2 matrix	10	—	22.7	—	47	4	4.1	Pb	34
Functionalized halloysite nanotubes	7	0.5	23.58	—	0.32	—	3.4	Pb	2
Diethylenetriamine-functionalized carbon nanotubes	30	1.5	5.4	75	0.16	—	3	Cr, Fe, Pb and Mn	35
A new chelating resin	—	4	18.3	200	1.9	—	—	Fe, Zn, Cu, Cr, Co and Mn	36
4-Aminoantipyrine immobilized bentonite	—	2	38.8	100	0.12	—	2.7	Cr, Hg and Pb	37
The new surface-imprinted activated carbon sorbent for Pb(II)	15	3	35.33	200	0.18	8	2.2	Pb	This work

[a] Equilibrium time. [b] Flow rate. [c] Enrichment factor.

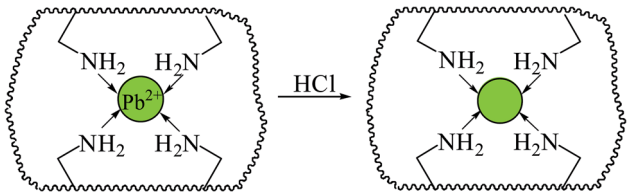

Fig. 12 Proposed reaction mechanism for Pb(II)-adsorption.

a compound with a coordination number of four. The IIP was tailored to the template Pb(II). Other metal ions could chelate with the nitrogen atoms of IIP, but they did not fit the tailored material. Therefore, IIP had a selectivity only for Pb(II). According to the selectivity experiment, the selectivity was controlled by the shape of the cavities (the size of the metal ions) and the coordination-geometry.[34]

The influences of pH and the initial concentration of Pb(II) on the adsorption rate suggested that there was a competitive adsorption of Pb(II) and H^+ to the nitrogen atoms. At low pH, the nitrogen atoms would be protonated, which would repel the positively charged Pb(II) ions. Therefore, the chelation performance decreased with the decreasing of pH and this is the reason why HCl could achieve effective elution in this experiment.

Conclusions

Ion-imprinted sorbents have attracted widespread attention as highly selective sorbents for the selective removal of target metal ions in the presence of other metal ions. In this study, we have firstly synthesized a new surface-modified Pb(II)-IIP, incorporating ethylenediamine as the chelating unit. The test data from FT-IR, XRD, SEM and BET proved that the synthesis of Pb(II)-IIP was successful. The prepared Pb(II)-IIP could be applied to selectively extract or separate Pb(II) ions from environmental samples containing foreign coexisting ions. The adsorption process could be described well by the pseudo-second-order model and Langmuir isotherm model. In addition, this adsorbent showed a number of good characteristics such as high chemical stability, excellent reproducibility, high adsorption capacity, high enrichment capability, high selectivity, and fast adsorption and desorption kinetics. As a conclusion, the Pb(II)-IIP prepared in this work can be considered to be a suitable and reliable sorbent for the separation and pre-concentration of Pb(II) ions in environmental water samples.

Conflicts of interest

There are no conflicts to declare.

Acknowledgements

This work was supported by the Fundamental Research Funds for the Central Universities, Northwest Minzu University (No. 31920180040; No. zyz2012065) and the National Natural Science Foundation of China (No. 31760608; No. 21762038).

References

1 B. Zargar and A. Khazaeifar, *Microchim. Acta*, 2017, **184**, 4521–4529.
2 Q. He, D. Yang, X. Deng, Q. Wu, R. Li, Y. Zhai and L. Zhang, *Water Res.*, 2013, **47**, 3976–3983.
3 N. Li, H. L. Jiang, X. Wang, X. Wang, G. Xu, B. Zhang, L. Wang, R. S. Zhao and J. M. Lin, *TrAC, Trends Anal. Chem.*, 2018, **102**, 60–74.
4 C. F. Poole, *TrAC, Trends Anal. Chem.*, 2003, **22**, 362–373.
5 Y. Matsui, S. Nakao, A. Sakamoto, T. Taniguchi, L. Pan, T. Matsushita and N. Shirasaki, *Water Res.*, 2015, **85**, 95–102.
6 D. Li, X. Chang, Z. Hu, Q. Wang, Z. Tu and R. Li, *Microchim. Acta*, 2011, **174**, 131–136.
7 M. Song, Y. Wei, S. Cai, L. Yu, Z. Zhong and B. Jin, *Sci. Total Environ.*, 2018, **618**, 1416–1422.
8 A. Macías-García, M. Gómez Corzo, M. Alfaro Domínguez, M. Alexandre Franco and J. Martínez Naharro, *J. Hazard. Mater.*, 2017, **328**, 46–55.
9 M. Ghaedi, H. R. Noormohamadi, A. Asfaram, M. Montazerozohori and M. Soylak, *J. Mol. Liq.*, 2016, **221**, 748–754.
10 X. F. Zheng, Q. Lian and H. Yang, *RSC Adv.*, 2014, **4**, 42478–42485.
11 W. Han, L. Gao, X. Li, L. Wang, Y. Yan, G. Che, B. Hu, X. Lin and M. Song, *RSC Adv.*, 2016, **6**, 81346–81353.
12 J. Tan, Z. Jiang, R. Li and X. Yan, *TrAC, Trends Anal. Chem.*, 2012, **39**, 207–217.
13 H. H. Yang, S. Q. Zhang, W. Yang, X. L. Chen, Z. X. Zhang, J. G. Xu and X. R. Wang, *J. Am. Chem. Soc.*, 2004, **126**, 4054–4055.
14 K. Haupt, *Analyst*, 2001, **126**, 747–756.
15 G. Wulff, *Angew. Chem., Int. Ed. Engl.*, 1995, **34**, 1812–1832.
16 K. Ensing and T. Boer, *TrAC, Trends Anal. Chem.*, 1999, **18**, 138–145.
17 Y. Liu, X. Chang and S. Wang, *Anal. Chim. Acta*, 2004, **519**, 173–179.
18 J. Qian, S. Zhang, Y. Zhou, P. Dong and D. Hua, *RSC Adv.*, 2015, **5**, 4153–4161.
19 F. Shakerian, K. H. Kim, E. Kwon, J. E. Szulejko, P. Kumar, S. Dadfarnia, A. Mohammad and H. Shabani, *TrAC, Trends Anal. Chem.*, 2016, **83**, 55–69.
20 H. He, Q. Gan and C. Feng, *RSC Adv.*, 2017, **7**, 15102–15111.
21 J. Wang, C. Jiang, X. Wang, L. Wang, A. Chen, J. Hu and Z. Luo, *Analyst*, 2016, **141**, 5886–5892.
22 R. Garcia, C. Pinel, C. Madic and M. Lemaire, *Tetrahedron Lett.*, 1998, **39**, 8651–8654.
23 H. T. Tang, *Organic Compound Spectra Determination*, Publishing House of Bei-jing University, Beijing, 1992, pp. 124–59.
24 Q. N. Dong, *IR Spectrum Method*, Publishing House of the Chemical Industry, Beijing, 1979, pp. 104–168.
25 Y. Liu, L. H. Zhu, Y. Y. Zhang and H. Q. Tang, *Sens. Actuators, B*, 2012, **171–172**, 1151–1158.

26 H. Meng, Z. Li, F. Ma, X. Wang, W. Zhou and L. Zhang, *RSC Adv.*, 2015, **5**, 67662–67668.
27 P. Yuan, P. D. Southon, Z. W. Liu, M. E. R. Green, J. M. Hook, S. J. Antill and C. J. Kepert, *J. Phys. Chem. C*, 2008, **112**, 15742–15751.
28 J. J. Wang and X. Li, *Ind. Eng. Chem. Res.*, 2013, **52**, 572–577.
29 G. Z. Fang, J. Tan and X. P. Yan, *Anal. Chem.*, 2005, **77**, 1734–1739.
30 A. Maquieira, H. Elmahadi and R. Puchades, *Anal. Chem.*, 1994, **66**, 3632–3638.
31 R. S. A. Machado, J. M. G. Fonseca, L. N. H. Arakaki, J. G. P. Espinola and S. F. Oliveira, *Talanta*, 2004, **63**, 317–322.
32 X. Zhu, Y. Cui, X. Chang, X. Zou and Z. Li, *Microchim. Acta*, 2009, **164**, 125–132.
33 E. Yavuz, Ş. Tokalıoğlu, H. Şahan and Ş. Patat, *Talanta*, 2013, **115**, 724–729.
34 C. Li, J. Gao, J. Pan, Z. Zhang and Y. Yan, *J. Environ. Sci.*, 2009, **21**, 1722–1729.
35 X. Zhu, Y. Cui, X. Chang and H. Wang, *Talanta*, 2016, **146**, 58–363.
36 Ş. T. Daşbaş, N. Çankaya and C. Soykan, *Food Chem.*, 2016, **211**, 68–73.
37 Q. Wang, X. Chang, D. Li, Z. Hu, R. Li and Q. He, *J. Hazard. Mater.*, 2011, **186**, 1076–1081.